Focal plane analysis of the Knox-Thompson algorithm in speckle interferometry

S.N. Karbelkar[1,2]

[1] Raman Research Institute, Bangalore 560080, India
[2] Joint Astronomy Programme, Physics Department, Indian Institute of Science, Bangalore 560012, India

Abstract. For the specific case of binary stars we present signal to noise ratio (SNR) calculations for the detection of the parity (the side of the brighter component) of the binary using the double correlation method. This double correlation method is a focal plane version of the well-known Knox-Thompson method used in speckle interferometry. We show that SNR for parity detection using double correlation depends linearly on binary separation. This new result was entirely missed by previous analytical calculations dealing with a point source. We conclude that for magnitudes relevant to the present day speckle interferometry and for binary separations close to the diffraction limit speckle masking has better SNR for parity detection.

Key words: speckle interferometry – image processing – seeing

1. Introduction

In ground based high resolution astronomy (for a recent review see Roddier, 1988) one is faced with problems of imaging astronomical objects through the Earth's turbulent atmosphere. Instantaneous focal plane image of a point source (PSF) is about one arcsec wide, irrespective of the diameter of the telescope so long as it is larger than 10 cm. The image contains many bright spots the so called speckles with nearly diffraction limited size. The goal of speckle interferometry, pioneered by Labeyrie (1970), is to reconstruct high resolution images from (perhaps) a large number of short exposure (~ 10 ms) images. Although the focal plane image of a point source is quite random two nearby point sources produce almost the same image apart from overall brightness and shift. This so called isoplanatic patch, within which the light from two objects encounters nearly the same atmospheric turbulence and thus produce similar images, is typically ten arcsecond wide in the optical. The stochastic nature of the PSF forces one to use statistical methods of image reconstruction. Labeyrie (1970) proposed and Gezari et al. (1972) successfully demonstrated the use of the power spectrum

$$\langle I_u I_{-u} \rangle = \langle R_u R_{-u} \rangle S_u S_{-u} \tag{1a}$$

$$I_u = \int \mathrm{d}^2 x e^{iux} I(x) \tag{1b}$$

in measuring stellar diameters. Here I_u, R_u and S_u are Fourier components of the observed focal plane intensity $I(x)$, the point

spread function $R(x)$ and the source structure $S(x)$ respectively; the angle brackets denote the average over atmospheric fluctuations. Theoretical estimates of the SNR for the power spectrum method suggest that the limiting magnitude of the technique is around 20^m (Dainty, 1974). However, this technique does not yield the phases of the Fourier components S_us which are necessary for unambiguous reconstruction of the source structure $S(x)$. Two promising phase recovery schemes exist. In the phase recovery scheme proposed by Knox and Thompson (1974, KT) one measures the second order correlation

$$\langle I_u I_{-u+\Delta u} \rangle \tag{2}$$

which is nonzero if $\Delta u < \Delta u_{max} \sim r_0/\lambda f$ where r_0 is the Fried parameter (~ 10 cm). This second order statistic contains information about the gradient $\nabla_u S_u$ of the source structure. The actual phases are obtained from these gradients recursively. Weigelt (1977) proposed another technique, the speckle masking, which uses the triple correlation (TC) (also known as the bispectrum)

$$\langle I_u I_v I_{-u-v} \rangle = \langle R_u R_v R_{-u-v} \rangle S_u S_v S_{-u-v}. \tag{3}$$

Although in this case also one has to solve for S_us recursively the $u-s$ and $v-s$ can take any values right up to the diffraction limit of the telescope.

The purpose of this paper is to point out certain subtle features of the KT technique that are unimportant in the TC method. These special features of the KT method were missed in the previous works. Nisenson et al. (1983) considered the effect of photon noise on speckle image reconstruction with the Knox-Thompson algorithm. Ayers et al. (1988) consider the full four dimensional extension of the KT algorithm in addition to using better description of the photon noise and atmospheric statistics. Chelli (1988) has derived analytic expressions for phase errors in one and two dimensions. However, these papers deal only with a point source. For a point source the phases of the Fourier components of the source structure deal with the location of the source. Estimating these phases and the error on them is of little importance. What is more important is that part of the phase information which can remove the structural ambiguities present in the autocorrelation analysis. Technically, it is not enough to consider the SNR only for the Knox-Thompson correlation for the system response R_us. In addition to the SNR for the point source correlation SNR for any technique involves a factor that depends on the source structure S_u. This dependence is not very

dramatic in the case of TC (Karbelkar, 1990c). To be specific, we consider a binary star (whose individual components are unresolved) with component's fluxes α_1 and α_2 and the separation b. In the case of binaries the only ambiguity that is left over after measuring its autocorrelation is its parity (defined as the side of the brighter component). Binary stars are perhaps the simplest sources for which some ambiguity (180° in position angle) remains after measuring the power spectrum. Parity is known to the binary star observers as quadrant ambiguity. Parity is important in some astronomical applications, examples being the recently discovered 'companion' to SN 1987 A and closely separated gravitational lens images. Quadrant ambiguity may play crucial role in determining the orbital parameters for a binary as in the case of 70 Tauri (Mc Alister et al., 1988). Although it is known that for a binary with widely separated components first order method can be used, nevertheless, it is useful to consider binaries in the context of double and triple correlation for two reasons. First of all, the simple nature of the object allows explicit SNR calculations in the image plane for these techniques. Secondly, a comparison of various techniques is more straightforward in the case of a binary as one is directly dealing with a property of the object itself rather than intermediate quantities like the phase gradient or the triple correlation. Although the more relevant phases of the object distribution are built up from these there is, so far, no explicit analytic connection between the SNR for these intermediate quantities and the final phase errors. The principal difficulty lies in the fact that given the phase gradient (with different individual noises) the final phases can be obtained in many different ways and the optimum solution is not expressible analytically. Existing SNR calculations for the phase errors use very plausible improvement factors which connect the SNR for the intermediate quantities to the final phase errors. Karbelkar (1990a, c) has estimated SNR for parity detection using TC. Although the SNR depends on the fluxes α_1 and α_2 it does not strongly depend on the binary separation b so long as it is smaller than the seeing.

In this paper we show that the SNR for parity detection using double correlation depends linearly on the binary separation (for separations close to the diffraction limit). It is only in the limit that the separation approaches the seeing that the SNR for KT becomes comparable to that of the power spectrum analysis. As a consequence of this dependence KT has poorer SNR for parity detection than the TC in spite of it being a lower order statistics. The advantage due to the lower order statistics shows for magnitudes greater than 18^m. This result is contrary to the existing analytic calculations which use a point source as representative. In Sect. 2 we present our analytical estimates for parity detection using double correlation. Numerical results are presented in Sect. 3 while the details are left to the appendices.

2. Parity detection using double correlation

2.1. Motivation

Our motivation for considering parity detection using double correlation is as follows. The crucial point in the KT method is the restriction $\Delta u < \Delta u_{max}$. The pupil plane length scale r_0 gives rise to the seeing disk of size $\sigma = \lambda f / r_0$ in the focal plane. If r_0 were zero then the seeing disk would be infinite in comparison to the speckle size $\rho = \lambda f / D$ rendering the KT method useless. In the limit $r_0/D \to 0$ the focal plane pattern due to a point source will

become stationary (statistically invariant under shifts) in the focal plane. If any process is stationary then the only nonzero second order correlation is the power spectrum which does not contain any phase information. In reality, the finite size of the seeing disk saves the situation by breaking the stationarity in the focal plane. Note that the bispectrum, on the other hand, is a special case of the most general triple correlation $\langle I_u I_v I_{-u-v+\Delta u} \rangle$ with $\Delta u = 0$. It is, therefore, meaningful even in the limit $r_0/D \to 0$.

For a binary within an isoplanatic patch the focal plane image consists of two similar speckle patterns due to the two stars forming the binary. Different speckles due to the same star have uncorrelated intensities, however, for every speckle due to star 1 there is one speckle due to the star 2 which has the same relative intensity and separation as the true binary. Any information about the binary must come from these correlated pairs of speckles (otherwise one can be happy with the long exposure image). Above, we argued that for KT to work finite size of the seeing disk is a must. The statistics of speckles change on the scale σ of the seeing disk and this change must be felt by the correlated pairs of speckles with separation b. We, therefore, expect a small parameter b/σ in the SNR for parity detection using double correlation which goes to zero smoothly as $(b/\sigma) \to 0$. This physical interpretation explains the existence and the crucial importance of the restriction $\Delta u < \Delta u_{max}$ required by this technique. Before presenting the details of focal plane calculations we give frequency domain arguments to show that this small parameter should also be present in the SNR expression for phase determination for objects small compared to the seeing disk.

2.2. Frequency domain estimates

The double correlation used in KT method can be expanded in a Taylor series as follows

$$\langle I_u I_{-u+\Delta u} \rangle = \langle I_u I_{-u} \rangle + \Delta u \cdot \langle R_u R_{-u} \rangle S_u \nabla_u S|_{-u} + \Delta u \cdot \langle R_u \nabla_u R|_{-u} \rangle S_u S_{-u} + O(\Delta u^2). \tag{4}$$

The first term is just the power spectrum $\langle I_u I_{-u} \rangle$. The third term contains only the power spectrum of the source and not its phase. Only the second term contains phase information. Also note that both the second and the third terms depend on the choice of the origin, in the focal plane, through the gradient. Since the second term contains phase information we show the origin dependence explicitly. Let the binary be

$$S(x) = \alpha_1 \delta(x - x_1) + \alpha_2 \delta(x - x_2)$$

or

$$S_u = \alpha_1 e^{iux_1} + \alpha_2 e^{iux_2} \tag{5}$$

where α_1 and α_2 are the relative fluxes of the components situated at x_1 and x_2 respectively. If $b = x_2 - x_1$ is the binary separation then the flux center x_c is $(\alpha_1 x_1 + \alpha_2 x_2)/(\alpha_1 + \alpha_2)$. With this, the second term (apart from $\langle R_u R_{-u} \rangle$) becomes

$$\Delta u \cdot S_u \nabla_u S|_{-u} = i\Delta u \cdot x_c(\alpha_1^2 + \alpha_2^2 + 2\alpha_1\alpha_2 \cos ub)$$

$$- i\frac{\alpha_1\alpha_2(\alpha_1 - \alpha_2)}{\alpha_1 + \alpha_2}\Delta u \cdot b + i\frac{\alpha_1^2\alpha_2}{\alpha_1 + \alpha_2}e^{-iub}\Delta u \cdot b$$

$$- i\frac{\alpha_1\alpha_2^2}{\alpha_1 + \alpha_2}e^{iub}\Delta u \cdot b. \tag{6}$$

Note that the coefficient of the flux center x_c is the power spectrum of the binary. In general, although the second term depends on the choice of the focal plane origin, the origin dependent contribution is the power spectrum. The KT signal *proper* comes when the flux center is chosen as the origin. Although the first term in Eq. (4) is noisy it is purely real by construction and cannot contaminate the purely imaginary part of the KT signal [for example the second term in Eq. (6)]. The noise on this comes from the third term of Eq. (4). Since all origin shifts can be attributed to the source structure, without any loss of generality, we origin the system response at the flux center so that in $\Delta u \cdot \langle R_u \nabla_u R|_{-u}\rangle$ origin dependent term analogous to the first term in Eq. (6) is absent. R_u and $\nabla_u R|_{-u}$ can be regarded uncorrelated and thus $\langle R_u \nabla_u R|_{-u}\rangle$ vanishes. However, $\langle |R_u \nabla_u R|_{-u}|\rangle \sim \langle R_u R_{-u}\rangle / \Delta u_{max}$ as $\Delta u_{max} = r_0/\lambda f = 1/\sigma$ is the correlation length for R_u. Thus the noise on $\langle R\nabla R\rangle$ is the same as that for the usual power spectrum. We emphasize that the $b \cdot \Delta u$ dependence is true for all light levels. The SNR for KT method is b/σ times poorer than the corresponding SNR for the power spectrum method:

$$SNR_{phase} \sim (b/\sigma) SNR_{power\ spectrum}, \qquad (7)$$

$$SNR_{parity} \sim (b/\sigma) SNR_{autocorrelation}. \qquad (8)$$

Equation (8) follows from Eq. (7) since information about the parity is contained in $N_s \sim (D/r_0)^2$ independent phases. The situation is similar to the autocorrelation for the binary which has SNR better than individual power spectrum values. Supplementing these results by the known results for the autocorrelation method (Dainty, 1974; Dainty, and Greenaway, 1979) we get the SNR for the KT method

$$SNR_{phase} \sim (b/\sigma) \quad \text{high flux}, \qquad (9a)$$

$$\sim (b/\sigma)\mathcal{N} \quad \text{low flux } \mathcal{N} < 1, \qquad (9b)$$

$$SNR_{parity} \sim (b/\sigma)N_s^{1/2} \quad \text{high flux}, \qquad (10a)$$

$$\sim (b/\sigma)N_s^{1/2}\mathcal{N} \quad \text{low flux } \mathcal{N} < 1, \qquad (10b)$$

where $\mathcal{N}$ is photon count per speckle in an exposure and $N_s \sim D^2/r_0^2$ is the average number of speckles in the PSF. In the following sections we support these frequency domain arguments by explicit analytic calculation for the SNR for parity detection using double correlation. The results agree with the scalings given above. We also note that the factor b/σ is about $N_s^{-1/2}$ for binaries close to the diffraction limit.

2.3. SNR for parity detection using double correlation

Our method is as follows. First we calculate the general double correlation PSFDC for the point spread function (PSF). This PSFDC turns out to be inversion symmetric. The general double correlation for a binary is calculated next. It consists of four PSFDCs. The strength and locations of these four PSFDCs are asymmetric about the center of the binary double correlation. This leads to an asymmetry in the double correlation for the binary. Our aim is to locate those regions of the double correlation which contribute more to the asymmetry at the cost of minimum variance. To calculate PSFDC we need to assume the statistics obeyed by the pupil plane fields. We mimic atmospheric degradation by a single scale Gaussian correlation. In reality, departure from the single scale correlation is known to result in

drifting centroids of the instantaneous speckle pattern. We discuss this issue later on. In this paper we are not interested in correlation effects due to secondary Airy rings so use an apodized aperture to yield a Gaussian beam. The parity statistics P when defined will be of the form

$$P = \int d^2x d^2y\, W(x,\ y)\langle I(x)I(y)\rangle \qquad (11a)$$

the sign of which tells us the parity of the binary. The lowest second order variance on this is given by

$$V = \int d^2x d^2y\, W(x,\ y)(W(x,\ y) + W(y,\ x))\langle I(x)I(y)\rangle. \qquad (11b)$$

A near optimum choice will be made for the weight function W so that the SNR is (apart from a numerical factor of the order unity) at its best. The parity signal, Eq. (11), is second order in the intensity and is evaluated for the single scale model. The variance of such a general double correlation involves terms second, third and fourth order in the intensity. In the case of autocorrelation method it is enough to consider only the lowest second order contribution if one is interested in "low" light levels. It is well-known that for autocorrelation method "low" light levels mean fainter than about 13^m when a speckle receives less than one photon in an exposure. Although it is obvious that even in the case of a general double correlation the second order terms should dominate at sufficiently "low" light levels it is not known what "low" means for a specific choice of the weight function.

Below we show that the PSFDC contains two features A and B. Both these features are capable of yielding parity information. The feature B, which is also the basis of the autocorrelation analysis, yields parity with better SNR than the feature A (basically long exposure). For feature A there are two transitions in the flux levels. The first transition occurs when a speckle receives less than one photon in an exposure. The second transition occurs when the entire telescope receives less than one photon in an exposure. Since this feature is not a genuine high resolution feature we evaluate its variance approximately (however, to all orders) in Appendix B. It is also shown, as a byproduct, in this appendix that for the usual autocorrelation and for parity detection using the feature B low light levels indeed mean fainter than 13^m. So for this feature we evaluate the variance only in the lowest order but using no further approximations than the single scale model already mentioned.

The connection between the focal plane approach taken here and the usual Fourier domain statement of the KT algorithm is seen clearly by substituting in the double correlation [Eq. (2)] the definition [Eq. (1b)] of a Fourier component. Individual KT Fourier domain correlation is then seen to be equivalent to

$$\int d^2x d^2y\, e^{iu(x-y)}e^{i\Delta uy}I(x)I(y).$$

The intensities $I(x)$ and $I(y)$ are correlated if x and y have a speckle in common i.e. $x \sim y$ or $y \pm b$. Thus the factor $\exp[iu(x-y)]$ can be pulled out of the integral. Since Δu is small we get the deviation of the individual KT correlation from its zeroth order power-spectrum relative in the form

$$\int d^2x\, xI(x)I(y).$$

478

To get the parity from individual KT correlations one has to, anyway, use different weights for different KT correlations so that there is nothing special about the linear weight. The weight function should only be inversion antisymmetric about the flux center.

2.3.1. The PSFDC

The focal plane is, of course, two dimensional. In the following we use x_1 and x_2 for focal plane coordinates. When we make one more copy of the focal plane the corresponding coordinates will be denoted by y_1 and y_2. As a result a general double correlation is four dimensional. In Fig. 1 the PSFDC is shown in the (x_1, y_1) plane. It consists of two features. The feature A has an extension of the order of the seeing disk and is shown symbolically by a circle. The feature B too has an extension of the order of the seeing disk but its width is just of the order of a speckle size
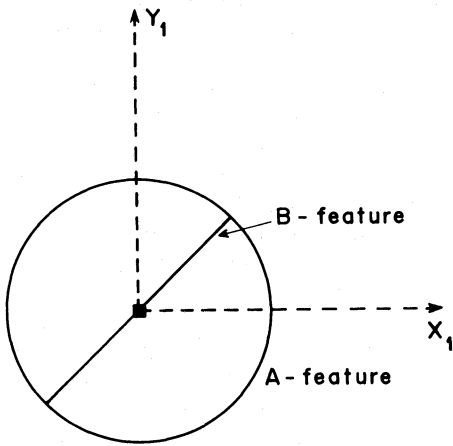

Fig. 1. Schematic representation of the PSFDC in the (x_1, y_1) plane. The feature A extends upto the circle of radius of the order of the seeing disk. The correlation ridge feature B exists only along the $+45°$ diagonal and has a width of the order of the speckle size. It is shown by a segment. The PSFDC is inversion symmetric about its center shown by a filled square

(shown by a segment along the $+45°$). In the full four dimensional space (x_1, x_2, y_1, y_2) the feature A is a four sphere while the feature B is a two dimensional layer. In our Gaussian model all these features have Gaussian fall offs with the above mentioned length scales. The two features have the same strength at the origin that can be readily estimated. With our normalization $\pi N_0 R^2$ is the total photon count per exposure for a zeroth magnitude star. This is distributed over the entire seeing disk of extent $\sigma \sim f/kl$ where $k = 2\pi/\lambda$ and l is the parameter of the single scale model (it is related to the Fried parameter r_0). Thus the average intensity density is $N_0 k^2 l^2 R^2/f^2$. The general double correlation depicted in Fig. 1 correlates intensity at two points in the focal plane. Now if these two points are separated more than a speckle size then their intensity fluctuations will be independent. For these regions the double correlation density will be the product of the two intensity densities. This is the reason for the term A whose strength is, therefore, $N_0^2 k^4 l^4 R^4/f^4$. Note that this feature is meaningful even for a long exposure image. Now consider those regions of the double correlation where the two points involved in the correlation are within a speckle size. This region is specified by the plane $x \sim y$ with a tolerance of the order of the speckle size. The intensity at these two points is correlated. Therefore, in this region there is excess correlation in addition to the term A. This excess is the term B. Note that this is a genuine high resolution feature: it does not exist for a long exposure image.

The double correlation for a binary is shown in Fig. 2. It contains four units of PSFDCs with strength and location shown in the figure. Because of the asymmetry in their strengths and locations, with respect to the center of the double correlation, the binary double correlation is asymmetric and one has to identify those regions of the double correlation which contribute significantly to the asymmetry. A more interesting question is to ask the relative importance of the two features of PSFDC in determining the parity of the binary. The answer to this question has implications for the more general question of optimum weight function. Intuitively one expects the optimum weight function to have two domains: one each for the two features of the PSFDC. The relative weight of the two domains determines what fraction of information is obtained from a specific feature. So one should, in principle, consider a weight function with two domains whose
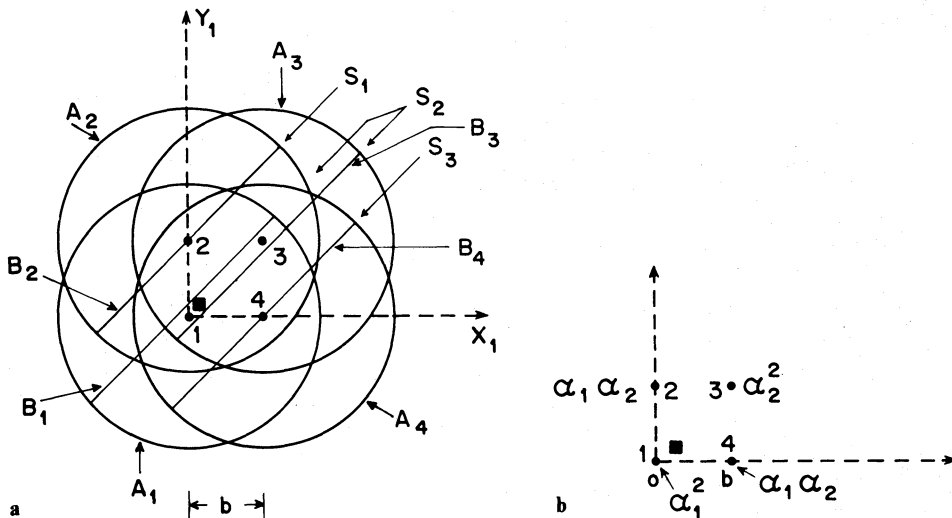

Fig. 2a and b. The general double correlation for a binary. The relative strengths of the four PSFDCs are shown in **b**. In the middle strip S_2 the features B_1 and B_3 should have passed through the dots 1 and 3 representing the centers of the first and the third PSFDCs and should therefore overlap. In the figure, for the sake of clarity of their extension, they are shown slightly displaced. The center of the binary double correlation is shown by a filled square

relative weights are such that the SNR for the resulting parity statistics is maximum. However, it is not necessary to carry out such a programme of parametric optimization. A kind of super-position approximation holds for the signal and the variance (but not for the SNR of course). Imagine that one knows the signal and the variance for the two features separately. Then the signal and the variance for any linear combination of the two features will be (approximately) the same linear combination of appropri-ate quantities for the individual features. This simplification owes its existence to the fact that the features A and B have vastly different four-volumes. If we take the four-volume of the feature B as unity (it actually contains N_S statistically independent regions) then the four-volume of the feature A is about $N_S = 2000$ (N_S^2 independent regions). For this reason, the difference between signal and noise due to the feature A and the feature A with voids of the size of the feature B is negligible.

It turns out that for binary separations close to the diffraction limit the feature B contributes dominantly to the parity while close to the seeing-sized separations parity is better determined by the feature A. So we consider two kinds of weight functions: one designed to emphasize the feature B and the second to emphasize the feature A. We give the order of magnitude scalings below while the details are left to the appendices.

Fig. 3. The weight function used to emphasize the feature B. It is nonzero only along the strips S_1, S_2 and S_3. The sign of the weight function is also shown

2.3.2. SNR for parity detection using feature B

In Fig. 2 we have taken the star 1 as the origin in the focal plane. We have aligned the axes so that the binary lies along the first axis. The center $(x_{c1}, x_{c2}, y_{c1}, y_{c2})$ of the entire double correla-tion is the same as the flux center of the long exposure image. The double correlation is, of course, four dimensional but for the planes (x_1, y_1) and (x_2, y_2) the center coordinates are the same as the corresponding components of the flux center of the long exposure image i.e. $x_{c1} = y_{c1} = b\alpha_2/(\alpha_1 + \alpha_2)$; $x_{c2} = y_{c2} = 0$. The center of the double correlation is shown by a filled square in Fig. 2. It is closer to the brighter star (which we take to be the star 1). We note from Fig. 2 that the correlation ridges (feature B) appear along three strips, labeled S_1, S_2 and S_3 in the figure, in the (x_1, y_1) plane. So our first choice of the weight function which emphasizes the feature B is one which is nonzero only along these three strips. The weight function is shown in Fig. 3. The strips have width equivalent to the feature B. The asymmetry in the double correlation about the flux center can be considered as asymmetry in the individual strips about a $-45°$ line passing through the flux center. This is because the middle strip passes through the flux center and therefore its one side becomes the other on inversion through the flux center. However, the upper part of the strip 1 becomes the lower part of the strip 3 on inversion through the center. But the strips 1 and 3 are identical in all realizations (because of the symmetry of the double correla-tion) so the lower part of the strip 3 can be replaced by the same as that of the strip 1. Thus one can talk about the asymmetry of the individual strips about the $-45°$ line passing through the center of the double correlation. In other words, one can com-pare the center (evaluated using the double correlation as the weight) of every $+45°$ strip in the double correlation with the point of intersection of this strip and the $-45°$ line passing through the center of the double correlation. The middle correla-tion ridge has its center displaced towards the brighter compon-ent of the binary while the other two strips have their centers shifted towards the fainter component by half the amount of the
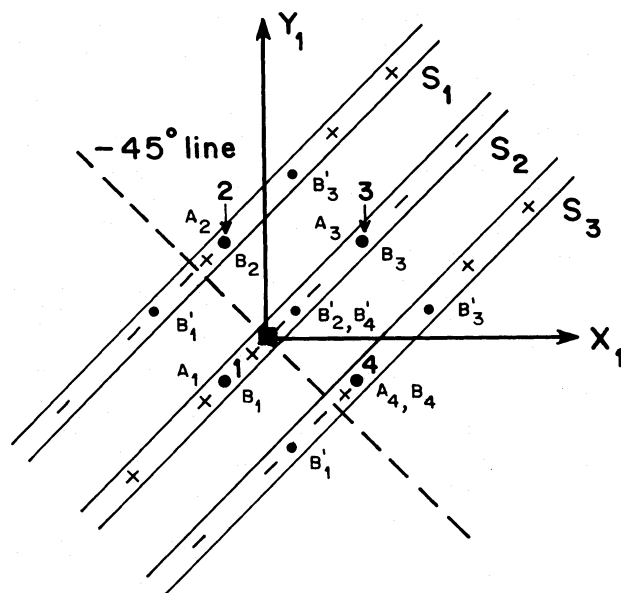
middle strip. Therefore, for these three strips taken together the center coincides with the flux center (the deviation appears in the third order in the binary separation). For any other $+45°$ strip consisting only in the feature A the center of the strip deviates from the $-45°$ line only in the third order in b and thus negligible for small separations. This motivates our weight function shown in Fig. 3. In this paper we have considered a very simple weight function which takes only three values: -1, 0, $+1$. In all figures the sign of the weight function is shown whereever it is nonzero. We emphasize that this simple choice should give SNR with correct scalings. In fact it is argued later on that although one can fine tune the weight function a bit one cannot improve the SNR by a factor much larger than unity and the scaling dependence of the SNR on N_S, b and $\mathcal{N}$ won't be affected.

Two points need to be clarified. The first point to note is that by definition the double correlation is symmetric in x and y for every realization of the atmospheric and photonic noise. There-fore, the strips 1 and 3 are identical. Our weight function, however, does draw information from both these strips. It can be shown that the SNR would have been the same if instead of using all the three correlation ridges we had used only the strip 1 and half (split along the plane $x = y$) of the middle strip. This is because although three strips give twice as much signal as would $1\frac{1}{2}$ strips the variance for three strips is four times larger than that for $1\frac{1}{2}$ strips. This is for the following reason. For weight func-tions which are nonzero only on one side of the plane $x = y$ only one term in Eq. (11b) contributes to the variance and that too half of what it would if the weight function were extended to the other side symmetrically. The second point to be noted is that the strips come with equal weights. Actually, one should weight the strips differently and work out the SNR for a choice of the relative weight. The relative weight is to be chosen so that the SNR is maximum. This question is best answered in the scheme which uses $1\frac{1}{2}$ strips. The variance due to the strip 1 and the

480

upper half of the middle strip is $\alpha_1^2 + 3\alpha_1\alpha_2 + \alpha_2^2$ and $\alpha_1^2 + \alpha_1\alpha_2 + \alpha_2^2$ respectively in proper units. The difference in the variance is not alarming especially when one is interested in binaries with widely different magnitudes of the components. It is well known that if two independent variables estimate the same quantity then the best linear combination is the one which weights the two variables by the reciprocal of their variance. Since the variances for the strips under consideration are nearly equal we consider equal weights for simplicity.

The order of magnitude scaling of the signal can be readily estimated. We note that if the binary separation were zero then there would be no asymmetry. For small separations the asymmetry is of the order of the binary separation b along the $+45°$ line. Now, we have seen before that the double correlation density is $N_0^2 k^4 l^4 R^4 / f^4$. To get the signal we must multiply this by the four volume equivalent of the asymmetry. Taking this to be of equivalent extension b and $\sigma \sim f/kl$ in the $x_1 = y_1$ plane and of the speckle size f/kR (remember there are two dimensions normal to this plane) normal to the plane we get the asymmetry in the double correlation to be $N_0^2 k l^3 R^2 b / f$. Indeed it is shown in Appendix A that the parity signal from all the three strips is

$$S_B = \frac{\pi^{1.5} N_0^2 k l^3 R^2 b \alpha_1 \alpha_2 (\alpha_1 - \alpha_2)}{2^{3.5} f(\alpha_1 + \alpha_2)}. \qquad (12a)$$

The low light level variance is obtained by simply multiplying the double correlation density and the entire four-volume of the feature B. It is shown in the Appendix A that the low light level variance is given by

$$V_B = \frac{1}{2}\pi^2 N_0^2 l^2 R^2 (\alpha_1 + \alpha_2). \qquad (12b)$$

Thus our estimate for the SNR for parity detection using the feature B is

$$\text{SNR}_B = \frac{4}{\sqrt{\pi}} q M^{1/2} \frac{\mathcal{N}_1 \mathcal{N}_2 (\mathcal{N}_1 - \mathcal{N}_2)}{(\mathcal{N}_1 + \mathcal{N}_2)^2} B \qquad (13)$$

where $\mathcal{N} = \pi l^2 N_0 \alpha / 16$ is the average photon count per speckle in an exposure, $B = kRb/2f$ is the binary separation in units of the diameter $\rho = 2f/kR$ of the PSF in the absence of atmospheric noise, q is the detector quantum efficiency (optics + detection) and M is the number of frames of data used. It may appear that only a fraction b/σ of the strips contributes to the signal. This is not true. For example the signal density along the central strip is (apart from overall strength) of the form

$$S(\eta) \propto \eta \exp[-k^2 l^2 \eta^2 / 8 f^2] \qquad (14)$$

where η is the coordinate along the strip. The signal density is obtained by taking the difference between the double correlation values at two points $\pm\eta$ away from the $-45°$ line. We see that the signal comes from all parts of the strip. If it were coming from some localized region then one could improve SNR by restricting the weight function to this area and thereby cutting down noise from regions with no or little signal. Thus the weight function chosen is near optimum and one can improve SNR only slightly by fine tuning the weight function but that should not affect the scaling with b and $\mathcal{N}$. Further improvement can be achieved by letting the weight function follow the signal. As one moves away from the center the photon noise will become more and more significant so the weight function should taper off to zero as one moves away instead of remaining constant. It can be shown that

instead of the step function kind of antisymmetric function if we had used a linear weight function (which is also antisymmetric) the SNR would have been $\sqrt{\pi}$ worse as this weight function gives more importance to regions farther away.

In autocorrelation analysis one is interested in getting the binary separation and one integrates along all $+45°$ strips. For the correlation ridges the result stands out relative to its neighbours.

2.3.3. SNR for parity detection using feature A

We now consider the asymmetry due to the uncorrelated regions of the double correlation. A representative weight function is shown in Fig. 4. As mentioned earlier the contribution to asymmetry is in the third order in the binary separation. A straight-forward calculation based on formulation given in Appendix A and for the weight function shown in Fig. 4 gives the parity contribution for this weight function:

$$S_A = \frac{\pi^{1.5}}{3 \cdot 2^{4.5}}[N_0^2 k^3 l^3 R^4 b^3 / f^3]$$

$$\times \frac{\alpha_1^2 \alpha_2^2 (\alpha_1 - \alpha_2) + \frac{1}{4}\alpha_1 \alpha_2 (\alpha_1 - \alpha_2)^2}{(\alpha_1 + \alpha_2)^3}. \qquad (15)$$

However, the noise calculation is not very straightforward because in the context of general weight function the term "low flux" needs qualification. In the Appendix B we show, using reasonable approximations that the variance for this weight function is given by

$$V_A = \frac{8}{3}N_s^3(\mathcal{N}_1 + \mathcal{N}_2)^4 + \frac{4}{3}N_s^3(\mathcal{N}_1 + \mathcal{N}_2)^3 + 2N_s^2(\mathcal{N}_1 + \mathcal{N}_2)^2. \qquad (16)$$

For this weight function there are two transition regions. The first one is when the dominant variance comes from the third order terms instead of the classical fourth order which dominate for bright sources. This happens around 11^m. The second transition occurs when the total flux is less than unity. The second order terms take over finally (18^m). The SNR for parity detection
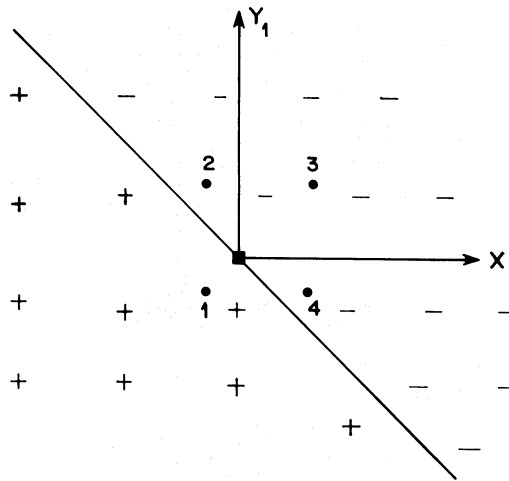

Fig. 4. The weight function used to emphasize the feature A

using the feature A is given by

$$\text{SNR}_A = \frac{8}{\sqrt{3\pi}} \frac{M^{1/2}}{N_S}$$

$$\times \frac{\mathcal{N}_1^2 \mathcal{N}_2^2 (\mathcal{N}_1 - \mathcal{N}_2) + \frac{1}{2}\mathcal{N}_1 \mathcal{N}_2 (\mathcal{N}_1 - \mathcal{N}_2)^2}{(\mathcal{N}_1 + \mathcal{N}_2)^5} B^3$$

high flux, (17a)

$$= \frac{8\sqrt{2}}{3\sqrt{\pi}} \frac{q^{1/2} M^{1/2}}{N_S}$$

$$\times \frac{\mathcal{N}_1^2 \mathcal{N}_2^2 (\mathcal{N}_1 - \mathcal{N}_2) + \frac{1}{2}\mathcal{N}_1 \mathcal{N}_2 (\mathcal{N}_1 - \mathcal{N}_2)^2}{(\mathcal{N}_1 + \mathcal{N}_2)^{4.5}} B^3$$

medium flux, (17b)

$$= \frac{16}{3\sqrt{\pi}} \frac{q M^{1/2}}{N_S^{1/2}}$$

$$\times \frac{\mathcal{N}_1^2 \mathcal{N}_2^2 (\mathcal{N}_1 - \mathcal{N}_2) + \frac{1}{2}\mathcal{N}_1 \mathcal{N}_2 (\mathcal{N}_1 - \mathcal{N}_2)^2}{(\mathcal{N}_1 + \mathcal{N}_2)^4} B^3$$

low flux. (17c)

We now show that although the feature A is a double correlation it is equivalent to a long exposure image. Let the intensity of the ith speckle sized pixel (see Appendix B for the physical motivation of this) be denoted by $\bar{n}_i$. In the regime the feature A dominates one can write the double correlation $\Sigma W_{ij} \langle \bar{n}_i \bar{n}_j \rangle$ approximately as $\Sigma W_{ij} \langle \bar{n}_i \rangle \langle \bar{n}_j \rangle$. We can think of this as equivalent to a first order statistics $\Sigma f_i \bar{n}_i$ where the equivalent weight function f_i is given by $f_i = \Sigma W_{ij} \bar{n}_j$. Now if we go to the flux center of the long exposure binary image then a constant weight function would give the total flux; a linear function would give zero (by definition of the flux center); a parabolic weight function would give the width of the image and thus can tell us the nonpoint nature of the source; a cubic weight function could give the parity. Now since W_{ij} is inversion antisymmetric f_i contains only odd powers of i in the average sense. So we see that our weight function is essentially playing the role of an equivalent i^3 in the case of first order parity statistics. In fact it is worse than that. The f_i has a fluctuating nature as opposed to the i^3 which is deterministic. In Appendix C we derive the SNR for parity detection using long exposure images.

3. Numerical results and discussion

Since there are two features to the PSFDC one can ask the following question. For a given brightness of the source what is the binary separation beyond which the parity is better determined by the feature A than the feature B. We do this for a binary with $\mathcal{N}_2 = (\mathcal{N}_1 - \mathcal{N}_2) = \frac{1}{2}\mathcal{N}_1$. This binary is expected to have better SNR as almost all SNR expressions have $\mathcal{N}_1 \mathcal{N}_2 (\mathcal{N}_1 - \mathcal{N}_2)$ in the numerator. Equating the two expressions for the SNR we find this separation to be

$$B = \frac{3}{2} q^{1/4} N_S^{1/2} \mathcal{N}_1^{1/4}. \tag{18}$$

This formula is valid for $2q\mathcal{N}_1 < 1$ (as we use low flux SNR for the feature B) and $\frac{2}{3} q N_S \mathcal{N}_1 > 1$ (as we use medium flux SNR for the feature A). When $\mathcal{N}_1 = 1$ we get $B = N_S^{1/2}$ i.e. the separation is

Table 1. Binary separation beyond which the feature A has a better SNR than the feature B for parity detection

Magnitude	14	15	16	17	18	19
Separation	34	26	21	17	13	10

equal to the seeing disk (this is a rather risky extrapolation of the Taylored calculations). As $\mathcal{N}_1$ decreases the binary separation for which the two features contribute equally also decreases. For a 4 m telescope, $q = 0.2$ we have given in Table 1 the values of B (the binary separation in units of speckle diameter ρ) for various magnitudes. It is evident from the table that the feature A is of little importance for binaries close to the diffraction limit.

Having shown the importance of the feature B in high resolution parity detection we now present SNR for parity detection using this feature. First of all letting $\mathcal{N}_2 = \frac{1}{2}\mathcal{N}_1$, we see that for reasonable observational parameters (10 ms exposure, 10^5 frames, 100 Å bandwidth, 4 m telescope diameter and detection efficiency 0.2) a SNR of 3 can be obtained for objects brighter than 14^m for separations close to the resolution limit. Also note from Eq. (13) that the SNR for fixed B does not depend on the telescope diameter. If in any technique individual speckles carry information then the SNR for such technique has a factor $N_S^{1/2}$ representing N_S independent elements of information. In the KT method, however, the small parameter b/σ masks this factor. In Table 2 we present the limiting magnitude of the fainter star for which parity can be determined using double correlation. This table also gives the limiting faintness for parity detection using the speckle masking method (Karbelkar, 1990a). Also the limiting magnitudes for parity detection using long exposure images, a result derived in the Appendix C, are given in this table. From the table we note that for separations close to the diffraction limit the speckle masking method has the best SNR. As the separation increases the KT method has better SNR. Finally, the long exposure image gives better SNR.

We have assumed that the flux center is a given quantity. It is well known that the flux center for every frame wanders in the focal plane and significant improvement is possible by aligning the centers of all the frames. The shift in the centroid is attributed to the turbulence scales larger than the Fried parameter (especially scales of the telescope size or larger). Refractive index scales on such large scales tilt the wavefront as a whole. The effect of these larger scales can, however, be mimicked by a larger value of σ for the following reason. Consider a short exposure frame. We can calculate the intensity double correlation for this frame. Now if we shift the image in the focal plane then the double correlation will also shift but the shift is along the 45° in the (x_1, y_1) plane. This is equivalent to a larger value of σ. Note that shifts in the focal plane do not diffuse the correlation ridges normal to their plane. This, of course, leads to a poorer SNR as the small parameter b/σ becomes smaller. Beletic (1988) in his numerical simulations finds the TC method to have better SNR than the KT method for complex sources. This he attributes to the wandering of the centroid of instantaneous image. As we have argued this is indeed true. The wandering makes the KT method poorer but that is not the entire truth. The main reason why the KT method is poorer for complex sources is the fact that this method depends on stationarity breakdown crucially and has a small source size parameter in its SNR.

482

Table 2. Limiting magnitude for parity detection using the long exposure (LE) image, the Knox-Thompson (KT) method and the triple correlation (TC) method. The limiting magnitude m_2 of the fainter star given as a function of the magnitude m_1 of the brighter component

m_1	Binary separation											
	1			4			7			10		
	LE	KT	TC	LE	KT	TC	LE	KT	TC	LE	KT	TC
13	X	16.2	17.2	16.5	17.7	17.2	18.5	18.2	17.2	19.5	18.7	17.2
14	X	15.7	17	16.5	17.7	17	19	18.2	17	20	18.7	17
15	X	X	16	16.5	17.7	16	19.5	18	16	20	18.7	16
16	X	X	X	X	X	X	19.7	18	X	20	18.7	X
17	X	X	X	X	X	X	20	X	X	20	X	X
18	X	X	X	X	X	X	20	X	X	20	X	X

Appendix A

The focal plane intensity $R(x)$ due to a point source (the PSF) is related to the pupil plane field $\varphi(\xi)$ by

$$R(x) = N_0 \left(\frac{k}{2\pi f}\right)^2 \int d^2\xi_1 d^2\xi_2$$
$$\times e^{i(k/f)x\cdot(\xi_1-\xi_2)}\varphi(\xi_1)\varphi^*(\xi_2)e^{-(\xi_1^2+\xi_2^2/2R^2)} \quad (A1)$$

where N_0 is normalization (see below), $k = 2\pi/\lambda, f$ is the focal length of the imaging system, $\exp-([\xi_1^2+\xi_2^2]/2R^2)$ is the apodization designed to give a Gaussian beam if the pupil plane input fields were not corrupted by the atmosphere. In that case $\varphi(\xi) = 1$ for a point source at the origin and the PSF $R_0(x)$ is given by

$$R_0(x) = N_0 \left(\frac{kR}{f}\right)^2 e^{-(k^2R^2x^2/f^2)}. \quad (A2)$$

The speckle diameter ρ is defined in terms of the equivalent area of the PSF

$$\frac{1}{4}\pi\rho^2 = \int d^2x e^{-(k^2R^2x^2/f^2)}, \quad \text{i.e.} \quad \rho = \frac{2f}{kR}. \quad (A3)$$

The normalization N_0 is the average photon count in an exposure per unit area due to a zeroth magnitude star i.e.

$$\int d^2x R_0(x) = N_0\pi R^2 \quad (A4)$$

gives the total number of photons passing through a telescope of radius R during one exposure time (bandwidth taken into account).

We assume that the pupil plane fields $\varphi(\xi)$ are stationary Gaussian fields with two point correlation function

$$\langle\varphi(\xi_1)\varphi^*(\xi_2)\rangle = e^{-4(\xi_1-\xi_2)^2/l^2}. \quad (A5)$$

With this pupil plane field statistics the long exposure PSF is given by

$$\langle R(x)\rangle = \frac{N_0 k^2 l^2 R^2}{16f^2} e^{-k^2l^2x^2/16f^2}. \quad (A6)$$

The equivalent diameter of this seeing is

$$\frac{1}{4}\pi\sigma^2 = \int d^2x e^{-k^2l^2x^2/16f^2} \quad \text{or} \quad \sigma = \frac{8f}{kl}. \quad (A7)$$

In this Gaussian model the average number of speckles N_S is

$$N_S = \frac{\sigma^2}{\rho^2} = 16\frac{R^2}{l^2}. \quad (A8)$$

For example, if the seeing is $1''$ the decorrelation length l defined by Eq. (A5) is 20 cm. A general correlation of any order can be obtained by the well known pairing theorem for Gaussian random variables (Reed, 1962). According to this rule the average of a high order correlation can be written down in terms of the two point correlation if the underlying distribution is Gaussian. To be more specific consider N random fields $\varphi_1, \ldots, \varphi_N$ and their conjugates $\varphi_1^*, \ldots, \varphi_N^*$. Then form N distinct pairs out of these $2N$ variables. Take the average of every pair. The average of the original $2N$-product is a sum of such paired products in every possible way. However, as every path in the Earth's atmosphere has a random path length of the order of hundreds of wavelengths in speckle interferometry further constraint can be imposed on the pairing rule. Every pair must have one φ and one φ^* as $\varphi_1\varphi_2$ has a completely random phase. Using this pairing theorem we get the PSFDC

$$\langle R(x)R(y)\rangle = \frac{1}{2^8}N_0^2\frac{k^4l^4R^4}{f^4}\left\{e^{-(k^2l^2/16f^2)(x^2+y^2)}\right.$$
$$\left. + e^{-(k^2R^2/2f^2)(x^2-y^2)}e^{-(k^2l^2/32f^2)(x+y)^2}\right\}. \quad (A9)$$

The first term is the term A and the second term is the term B. Now consider a binary with separation b and the relative strength α_1 and α_2 of the components

$$S(x) = \alpha_1\delta(x) + \alpha_2\delta(x-b) \quad (A10)$$

where we have chosen the focal plane origin to be the star 1. We also align the binary along the first axis. The general two point correlation for the binary contains four PSFDCs:

$$\langle I(x)I(y)\rangle = \alpha_1^2 \langle R(x)R(y)\rangle + \alpha_1\alpha_2 \langle R(x-b)R(y)\rangle$$
$$+ \alpha_1\alpha_2 \langle R(x)R(y-b)\rangle + \alpha_2^2 \langle R(x-b)R(y-b)\rangle. \tag{A11}$$

This correlation is shown in Fig. 2. Now consider the weight function of the first kind shown in Fig. 3. This has three strips whose width is equal to the width of the feature B. Consider the central strip. It contains B features due to the first and the third basic PSFDC unit. In addition it also covers part of the feature A due to all the four PSFDCs. The overlap of a A-feature and the weight function is equivalent to a B-feature. The centers of the second and the fourth PSFDCs do not lie on the central strip so the overlap of their A-features and the weight function is not exactly the same as that for the first and the third feature. However, as we are dealing with small binary separations we can take all such overlaps equal. The difference is in the third order in the binary separation. There are two reasons for this cubic deviation. One reason is that the maximum strength of an equivalent B feature falls off quadratically if the center of the A feature generating it does not lie on the strip. Secondly, the extension of the effective B feature also falls off quadratically. The correlations to the leading term are b^2 times smaller. So the central strip contains six equivalent B-features. Their strengths and centers are shown in Fig. 3. This figure also shows the contents of the other strips. We have shown equivalent B-features by a prime and the subscript tells us the PSFDC whose A-feature generated it. It is possible to project the double correlation on the $+45°$ line by integrating along the $-45°$ direction in the (x_1, y_1) plane and along the x_2 and y_2 directions as the weight function does not depend on them.

Let $\eta_1 = (x_1 + y_1)/2$ and $\xi_1 = (x_1 - y_1)/2$. Consider an equivalent B-feature whose center is η_c away from the jump in the weight function. Integrating along x_2, y_2 and ξ we get the signal and the variance due to one equivalent B-feature:

$$S = \frac{\pi^{1.5} N_0^2 k l^3 R^2 \beta}{2^{2.5} f} \int d\eta_1 w(\eta_1) \exp\left[-\frac{k^2 l^2}{8f^2}(\eta_1 - \eta_c)^2\right], \tag{A12}$$

$$V = \frac{\pi^{1.5} N_0^2 k l^3 R^2 \beta}{2^{4.5} f} \int d\eta_1 w^2(\eta_1) \exp\left[-\frac{k^2 l^2}{8f^2}(\eta_1 - \eta_c)^2\right], \tag{A13}$$

where $w(\eta_1)$ is the weight function along the $+45°$ line and β is the strength of the equivalent B-feature. For the representative weight function considered here the integral in (A12) is equal to the area of the central $\pm\eta_c$ part of the feature. For small binary separations this is well approximated by $2\eta_c$ into the projected correlation density. The contribution to the signal and the variance due to an equivalent B-feature is

$$S = \frac{\pi^{1.5} N_0^2 k l^3 R^3 \beta w(\eta_c)|\eta_c|}{2^{4.5} f}, \tag{A14}$$

$$V = \frac{\pi^2}{2^3} N_0^2 l^2 R^2 \beta. \tag{A15}$$

In the expression (A14) the factor $w(\eta_c)$ comes because depending on which side of the $-45°$ line the center is the contribution is $+ve$ or $-ve$. By summing up the contributions of the individual

effective B-features one get the signal and the noise for this weight function.

Appendix B: noise on a double correlation

As mentioned in the text the term "low light level" needs qualification in the case of a general weight function. It becomes necessary to consider the noise in all orders. Consider, then, a general second order statistics

$$\sum W_{ij} \bar{n}_i \bar{n}_j \tag{B1}$$

where $\bar{n}_i$ is the intensity on the i-th pixel. The noise on this statistics involves intensity correlations of second, third and fourth order. In order to avoid the task of dealing with field correlations of rather high order we use a simpler model of the PSF. In this model, we consider speckle-sized pixels so that intensities on the adjacent pixels can be considered independent. We assume that the intensity of a speckle is distributed according to the Rayleigh statistics (see Karbelkar, 1990a, for the details of the model used here). Another simplifying factor is that while considering the variance one can take a point source as representative. This is because the variance does not depend on the binary separation in its leading term. We, therefore, consider a point source with strength $(\alpha_1 + \alpha_2)$. Let $\bar{\mu}_i$ be the average photon count in an exposure due to a zeroth magnitude star. Calculation of noise on a correlation involves two steps. In the first step one removes the well-known photon bias from the statistics and then considers the atmospheric noise on the unbiased estimator. The problem of photon limited imaging was originally investigated by Goodman and Belsher (1976, 1977). In the following we use an algorithm which extends their results for a general weight function (Karbelkar, 1990b). The classical noise on the general double correlation is given by

$$V_4 = (\alpha_1 + \alpha_2)^4 \sum_{ijkl} W_{ij} W_{kl} [\langle \mu_i \mu_j \mu_k \mu_l \rangle - \langle \mu_i \mu_j \rangle \langle \mu_k \mu_l \rangle]. \tag{B2}$$

For the assumed statistical model for the μs the term in the classical variance can be shown to be [apart from $(\alpha_1 + \alpha_2)^4$]

$$V_4 = 8 \sum_{ijk} W_{ij} W_{ik} \langle \mu_i \rangle^2 \langle \mu_j \rangle \langle \mu_k \rangle + 8 \sum_{ij} W_{ij}^2 \langle \mu_i \rangle^2 \langle \mu_j \rangle^2$$
$$+ 8 \sum_{ij} W_{ij} W_{ii} \langle \mu_i \rangle^3 \langle \mu_j \rangle + 6 \sum W_{ii}^2 \langle \mu \rangle^4. \tag{B3}$$

In deriving this equation the symmetric nature of all the W's considered in this paper and the fact that two W's appear was used. We consider two kinds of weight functions. The first U_{ij} covers the cases of the autocorrelation and the one which stresses the contribution due to the feature B.

$$U_{ij} = F_i \delta_{ij}. \tag{B4}$$

For this weight function only one summation exists. Thus all terms in the classical fourth order variance are of the order of $N_S \mathcal{N}^4$. It will be shown later that for the weight function of the first kind the third order and the second order terms are of the order of $N_S \mathcal{N}^3$ and $N_S \mathcal{N}^2$ respectively. Thus for a weight function of this kind low flux means $\mathcal{N} < 1$ i.e. objects fainter than thirteenth magnitude. Now consider the weight function of the second kind shown in Fig. 4. The discrete analogue of which is

$$W_{i_1 i_2 j_1 j_2} = \text{sign}[i_1 + j_1] \tag{B5}$$

where we have written the vector subscript i in terms of its components and chosen i_1 along the binary. The components run from $-N_S^{1/2}/2$ to $+N_S^{1/2}/2$. This restriction actually comes from the fact that all correlations extend only up to the size of the order of the seeing disk. For this weight function it can be shown that

$$\sum_{j_1 j_2 i_2} = 2 i_1 N_S. \tag{B6}$$

Using this result it can be shown that the fourth order contribution to the variance is (apart from $(\mathcal{N}_1 + \mathcal{N}_2)^4$)

$$\left[\frac{8}{3}N_S^3 + 12 N_S^2 + 6 N_S\right]\mathcal{N}^4 \sim \frac{8}{3}N_S^3 \mathcal{N}^4. \tag{B7}$$

The third order variance is given by (Karbelkar, 1990b) [apart from $(\mathcal{N}_1 + \mathcal{N}_2)^3$]

$$V_3 = 4 \sum_{ijk} W_{ij} W_{ik} \left[\langle \mu_i \rangle \langle \mu_j \rangle \langle \mu_k \rangle + \delta_{ij} \langle \mu_i \rangle^2 \langle \mu_k \rangle \right.$$
$$\left. + \delta_{ik} \langle \mu_i \rangle^2 \langle \mu_j \rangle + \delta_{jk} \langle \mu_i \rangle \langle \mu_j \rangle^2 + 2 \delta_{ijk} \langle \mu_i \rangle^3 \right]. \tag{B8}$$

In deriving this the symmetric nature of all the W's used in this paper and the fact that two W's appear was used. Note that for the weight function of the first kind all terms are of the form $N_S \mathcal{N}^3$. Coming back to the weight function of the second kind it can be shown that the third order contribution to the variance is [apart from $(\mathcal{N}_1 + \mathcal{N}_2)^3$]

$$\left[\frac{4}{3}N_S^3 + 8 N_S^2 + 8 N_S\right]\mathcal{N}^3 \sim \frac{4}{3}N_S^3 \mathcal{N}^3. \tag{B9}$$

Similarly the second order contribution can be shown to be [apart from $(\mathcal{N}_1 + \mathcal{N}_2)^2$]

$$2[N_S^2 + N_S]\mathcal{N}^2 \sim 2 N_S^2 \mathcal{N}^2. \tag{B10}$$

Combining contributions to all orders we get the variance [Eq. (16)] for this weight function.

Appendix C: parity detection using long exposure image

While discussing the feature A we argued that it is equivalent to a long exposure image. Although it is not a genuine high resolution method we derive SNR for parity detection using long exposure images. We consider the first order statistics

$$S = \sum_{i_1 i_2} \left[i_1 - \frac{\alpha_2 b}{(\mathcal{N}_1 + \mathcal{N}_2)}\right]^3 \bar{n}_i \tag{C1}$$

where we have used the discrete pixel model used in the Appendix B. We have centered the cubic weight function on the flux center. The cubic nature follows because one is interested in the asymmetry in the long exposure image about the flux center (which is defined as the location where a linear weight function gives zero). A straight-forward calculation gives the signal and the variance

$$S_{LE} = N_S B^3 \frac{\mathcal{N}_1 \mathcal{N}_2 (\mathcal{N}_1^2 - \mathcal{N}_2^2)}{(\mathcal{N}_1 + \mathcal{N}_2)^3}, \tag{C2}$$

$$V_{LE} = \frac{N_S^4}{7 \cdot 2^6}\left[(\mathcal{N}_1 + \mathcal{N}_2)^2 + (\mathcal{N}_1 + \mathcal{N}_2)\right]. \tag{C3}$$

The SNR is given by

$$SNR_{LE} = 8\sqrt{7} M^{1/2} \frac{B^3}{N_S} \frac{\mathcal{N}_1 \mathcal{N}_2 (\mathcal{N}_1^2 - \mathcal{N}_2^2)}{(\mathcal{N}_1 + \mathcal{N}_2)^4} \quad \text{high flux,} \tag{C4}$$

$$= q^{1/2} 8\sqrt{7} M^{1/2} \frac{B^3}{N_S} \frac{\mathcal{N}_1 \mathcal{N}_2 (\mathcal{N}_1^2 - \mathcal{N}_2^2)}{(\mathcal{N}_1 + \mathcal{N}_2)^{3.5}} \quad \text{low flux.} \tag{C5}$$

References

Ayers, G.R., Northcott, M.J., Dainty, J.C.: 1988, *J. Opt. Soc. Am. A* **5**, 963

Beletic, J.W.: 1988, *ESO Conference and Workshop Proceedings No. 29*, ed. F. Merkle, p. 357

Chelli, A.: 1988, *ESO Conference and Workshop Proceedings No. 29*, ed. F. Merkle, p. 349

Dainty, J.C.: 1974, *Monthly Notices Roy. Astron. Soc.* **169**, 631

Dainty, J.C., Greenaway, A.H.: 1979, *J. Opt. Soc. Am.* **69**, 786

Gezari, D.Y., Labeyrie, A., Stachnik, R.V.: 1972, *Astrophys. J.* **173**, L1

Goodman, J.W., Belsher, J.F.: 1976, Publ. no. RADC-TR-76-50; RADC-TR-76-382; 1977, RADC-TR-77-175 (Rome Air Development Center) Griffiss Air Force Base, New York, 13441

Karbelkar, S.N.: 1990a, *Astrophys. J.* **351**, 334

Karbelkar, S.N.: 1990b, *J. Opt. Soc. Am. A* (to appear)

Karbelkar, S.N.: 1990c, *Astron. Astrophys.* **238**, 485

Knox, K.T., Thompson, B.J.: 1974, *Astrophys. J.* **193**, L45

Labeyrie, A.: 1970, *Astron. Astrophys.* **6**, 85

McAlister, H.A., Hartkoff, W.I., Bagnuolo, W.G.Jr., Sowell, J.R., Franzo, O.G., Evans, D.S.: 1988, *Astron. J.* **96**, 1431

Nisenson, P.J., Papaliolios, C.: 1983, *Opt. Commun.* **47**, 91

Reed, I.S.: 1962, *IRE Trans. Inf. Theory* **IT-8**, 194

Roddier, F.: 1988, *Phys. Rep.* **170**, 99

Weigelt, G.: 1977, *Opt. Commun.* **21**, 55